https://doi.org/10.46813/2026-165-171

A SOFTWARE PACKAGE FOR ANALYSIS OF PRODUCT PROCESSING REGIME AT AN ELECTRON ACCELERATOR

R. Pomatsalyuk, S. Romanovskyi, D. Titov, V. Tytov, V. Uvarov
National Science Center "Kharkiv Institute of Physics and Technology", Kharkiv, Ukraine
E-mail: rompom@kipt.kharkov.ua

The results of experimental study and computer simulation of the surface dose distribution as a function of width of the electron beam sweep and energy at an industrial accelerator LP-10 of NSC KIPT are presented. A developed Geant4 Monte Carlo model of the accelerator output devices is validated against the measurements. The simulated sweep widths agree with the experiment within 1…3%, while depth-dose distributions are matched with the independent data from other accelerators and with the ITS3 and Penelope codes.

PACS: 07.05.Tp, 29.20.Ej, 29.85.Fj, 29.27.-a

INTRODUCTION

Electron accelerators are used for industrial sterilizing the medical devices, pharmaceutical and food products, modifying the materials and treatment of the wastewater. Process efficiency depends strongly on the accuracy of the irradiation parameters: non-optimal regimes waste energy or can even degrade a product.

At processing with a scanning electron beam, the dose distribution on and inside an irradiated object is determined by beam energy and current, sweep width, and conveyor speed. Energy sets the penetration depth; current sets the dose rate; sweep width sets the uniformity and magnitude of the delivered dose. Optimizing these parameters ensures stable delivery of the target dose while improving the use of beam energy.

Some time ago, a software package on the basis of the PENELOPE-2008 transport code for modeling the processes in the objects of various geometry and composition exposed to a scanned electron beam had been developed [1]. The motivation of this work is an upgrade of that package to improve the accuracy of simulations because the new online methods of measuring the dose distribution, as well as new software and calculation techniques were developed and introduced during that period.

1. EXPERIMENTAL STUDY

1.1. METHOD

To characterize an industrial accelerator LP-10 of NSC KIPT [2], we measured the surface dose distribution as a function of sweep width and beam energy using a cathodoluminescence (CL) imaging technique [3], and also developed a Geant4 [4] Monte Carlo model of the accelerator output devices capable of analyzing and optimizing the processing parameters.

The width of the scanning-beam sweep on the irradiated object depends mainly on the electron energy and the magnetic field in the scanner gap, with an approximately linear relationship. Three measurement types were used:

• at constant beam energy and various preset sweep widths in the range 400…480 mm;

• at constant sweep width and various beam energy;

• at constant beam width and energy (to check radiator-to-radiator signal repeatability).

In all cases the conveyor speed was 2.2 cm/s, and the beam sweep parameters (profile, width, offset) were extracted from digital-camera images of the radiator's CL. Beam energy (mean E_{av} and most-probable E_p) was measured with a stack monitor (SM – [5]) before and after the irradiation. The CL radiator represented a 0.2 mm paper sheet fixed on a 1-mm aluminum plate by 59x26 cm in size. One RedPerspex 4034 PMMA dosimeter was mounted on every radiator at a distance of 17 cm from the lower edge of the transport container. Radiators were mounted on four containers, one container apart. The two CL images were recorded per radiator, as it passed under the beam. The profile, width and offset were restored with the purpose-built "CL-Profile" software system.

1.2. RESULTS

1.2.1. At a constant energy, the offset and width settings were chosen to provide the sweep signal offset at the generator output of 0 V, i.e. the beam was scanned symmetrically about its vertical center. The measured sweep width varied linearly with preset width and with scanner magnet current over the 400…480 mm range (Fig. 1, Table 1). The deviation between the two profiles of CL images used per radiator did not exceed 2%. Figs. 2, 3 shows the dependence of the measured sweep width on the scanner magnet current and on preset sweep width.

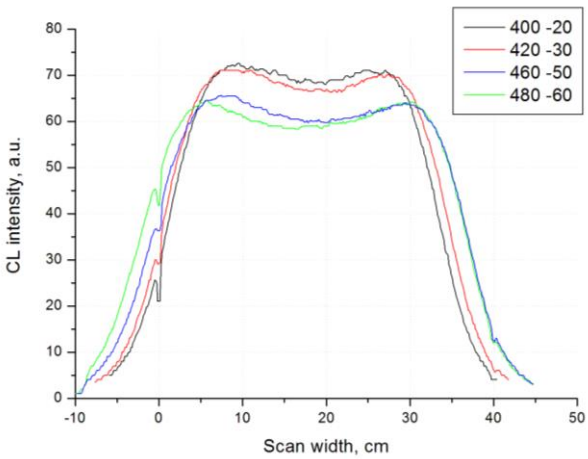


Fig. 1. Vertical sweep profiles for the four radiators at a different preset sweep width

Table 1

Accelerator parameters and measured sweep width (constant beam energy)

Preset width, mm	I, mA	Ep, MeV	Magnet I, A	Width, cm
400	0.778	9.71	13.5	24.8
420	0.775	9.72	14.65	26.7
480	0.772	9.73	16.5	31.5
460	0.773	9.71	15.8	29.7

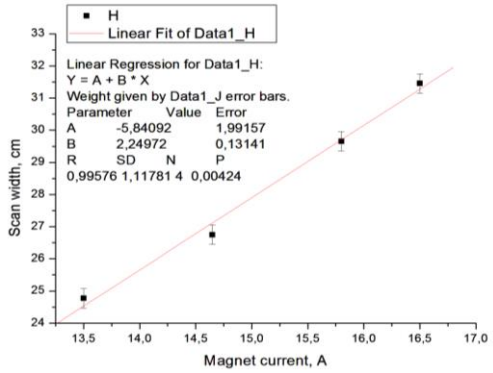


Fig. 2. Measured sweep width vs. scanner magnet current

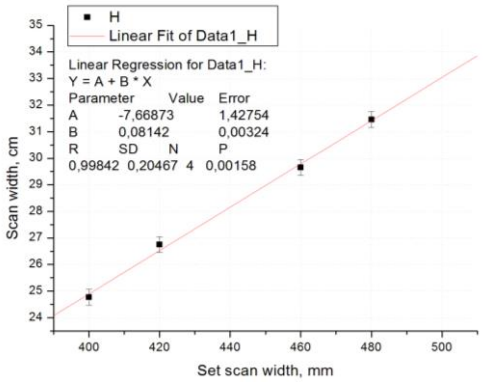


Fig. 3. Measured sweep width vs. preset sweep width

1.2.2. At a constant preset sweep width (460 mm), the CL signal intensity and the absorbed dose both depend on beam energy (Fig. 4). The sweep width on an object changes by ~2.8 cm per 1 MeV (Fig. 5, Table 2). The absorbed dose measured by RedPerspex dosimeters and normalized to beam current rose from 15.3 to 19.6 kGy/mA as E_p increased from 8.0 to 11.0 MeV (Fig. 6).

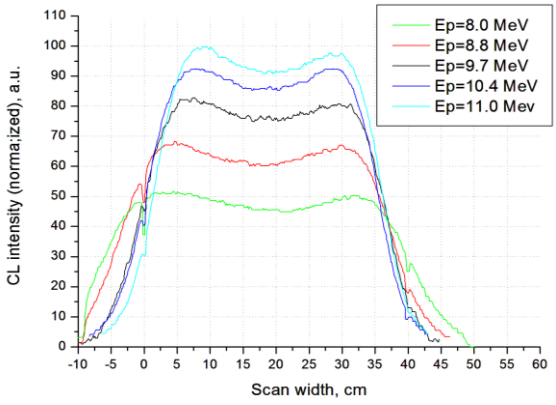


Fig. 4. Vertical sweep profiles (averaged over 2 frames) for the four radiators at different beam energies. CL signal intensity is normalized to mean beam current

Table 2

Sweep width and dose at different beam energies

Ep, MeV	I, mA	Width, cm	Dose, kGy	Norm. dose, kGy/mA
8.0	0.773	35.4	9.9	15.3
8.79	0.731	33.1	11.7	16.0
9.71	0.658	29.7	13.75	17.8
10.44	0.716	28.2	14.0	19.6
11.04	0.683	27.0	13.2	19.3

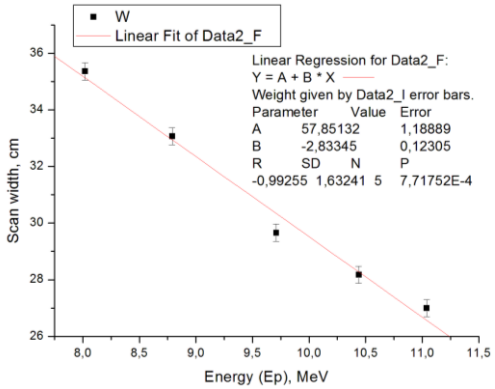


Fig. 5. Measured sweep width vs. most probable energy, Ep

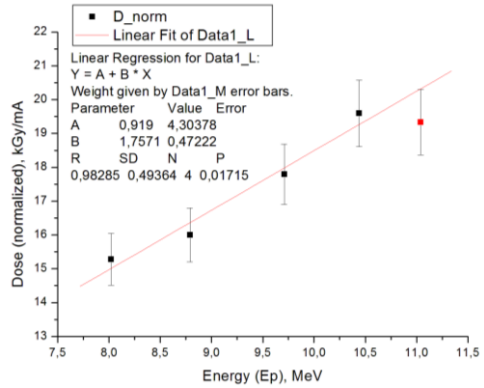


Fig. 6. Absorbed dose at different beam energies, normalized to beam current

Radiator-to-radiator repeatability at a fixed width/energy was within ~4% (Fig. 7).

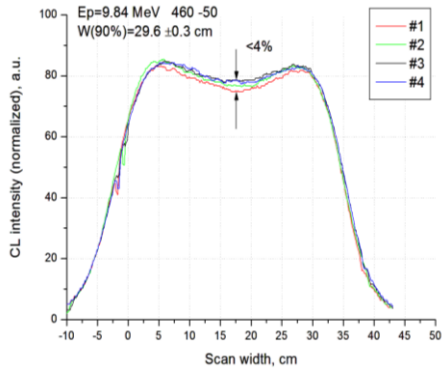


Fig. 7. CL signal intensity on four radiators at constant preset sweep width and constant beam energy (repeatability check)

2. SIMULATIONS

2.1. MODEL

A Geant4 transport code [4] was used to develop a computer model of the LP-10 output devices including a

scanning electromagnet, a 55-μm titanium exit window (5×50 cm), and also the target elements (Fig. 8). The energy spectrum of an electron source by 0.5-cm-in diameter was considered as a sum of the two Gaussians fitted to the real beam spectra [5] (Fig. 9), for E_p = 8…11 MeV. The scanner-magnet characteristics (Table 3) were adopted from [6]. The output-pole shape used in the simulation reproduces the real pole geometry (Fig. 10). An aluminum CL radiator (40×80×0.2 cm) is located at a distance of 91 cm from the accelerator exit window, followed by the phantom (80x40x38 cm) and, 230 cm downstream, a 10-plate aluminum stack monitor.

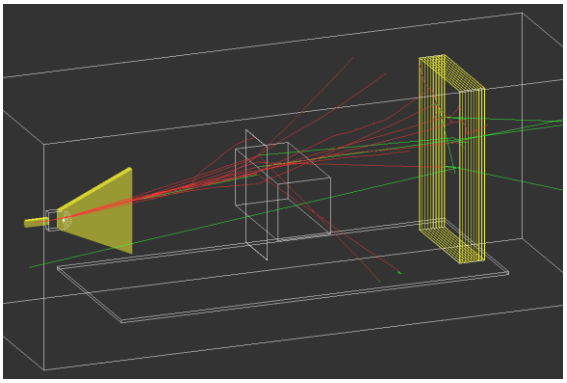


Fig. 8. Geometry of the LP-10 accelerator output devices used in simulations

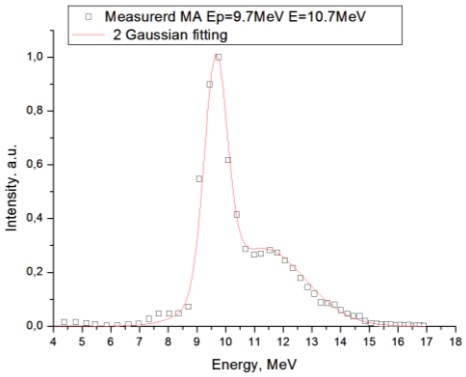


Fig. 9. Measured electron energy spectrum (squares) and its approximation by two Gaussians (line)

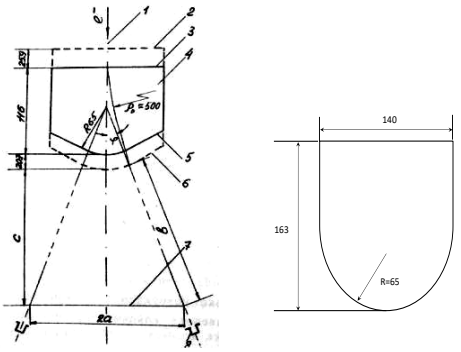


Fig. 10. On left – real scanner magnet pole, cm: a=20, b=50.25, c=46.7, φ=±20°; on right – the shape of the scanner-magnet output pole used in the simulations

The last represents an assembly of 10 aluminum plates with overall size of 122×75×19 cm (Y-height, X-width, Z-depth). The two outer plates are 5 mm thick; while the inner plates are 2 mm thick. The 20-mm air gaps separate adjacent monitor plates.

The simulations covered one scan period (0.33 s) with 10^5 electrons generated per pulse. The electron density distribution on the object was obtained as the sum of distributions of the individual beam pulses. A 125 Hz pulse repetition rate was set to reduce the computation time. The radiator plane was scored in 1×1×0.2 cm^3 cells and the phantom in 1×1×2 cm cells.

Table 3

Main characteristics of the beam and scanner

Parameter	Value
Electron energy, MeV	8...15
Max. sweep angle, deg.	± 20
Effective field length Ln, cm	16.26
Scanning frequency, Hz	1...3

An example of the results obtained using the simulation package is shown in Fig.11.

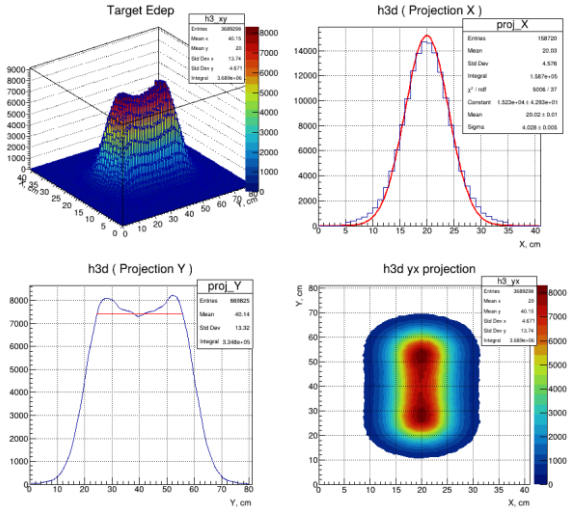


Fig. 11. Results of simulations Top-left and bottom-right: 2D distribution of absorbed energy in the aluminum radiator in the XY plane. Top-right: horizontal profile; bottom-left: vertical profile of the absorbed-energy distribution in the radiator

2.2. MODEL VALIDATION AGAINST BEAM MEASUREMENTS

The simulated beam sweep vs. scanner-magnet field reproduces their measured dependence (see Table 1) to within 1% (Table 4, Fig. 12).

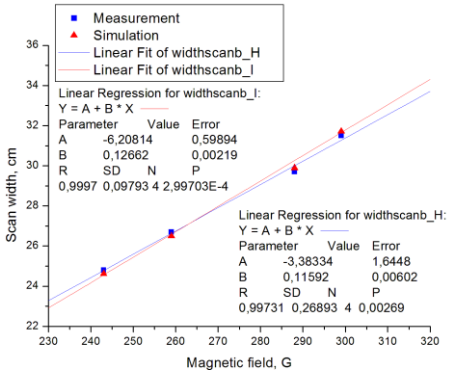


Fig. 12. Comparison of measured and simulated sweep width

Table 4

Measured and simulated sweep width vs scanner field

Field, G	Width, sim. cm	Width, meas. cm	Diff., %
243	24.6	24.8	-0.7
259	26.5	26.7	-0.7
288	29.9	29.7	1.0
299	31.7	31.5	0.7

Simulated sweep width vs. beam energy agrees with measurement to within 3% (Table 5). Simulated vertical and horizontal electron-flux profiles agree well with the CL-measured profiles once scaled to the measured maximum (Fig. 13).

Table 5

Measured vs. simulated sweep width vs. beam energy

Ep, MeV	Width, sim. cm	Width, meas. cm	Diff., %
8.0	35.5	35.4	0.3
8.8	32.9	33.1	-0.6
9.7	29.9	29.7	0.6
10.4	27.7	28.2	-1.8
11.0	26.4	27.0	2.3

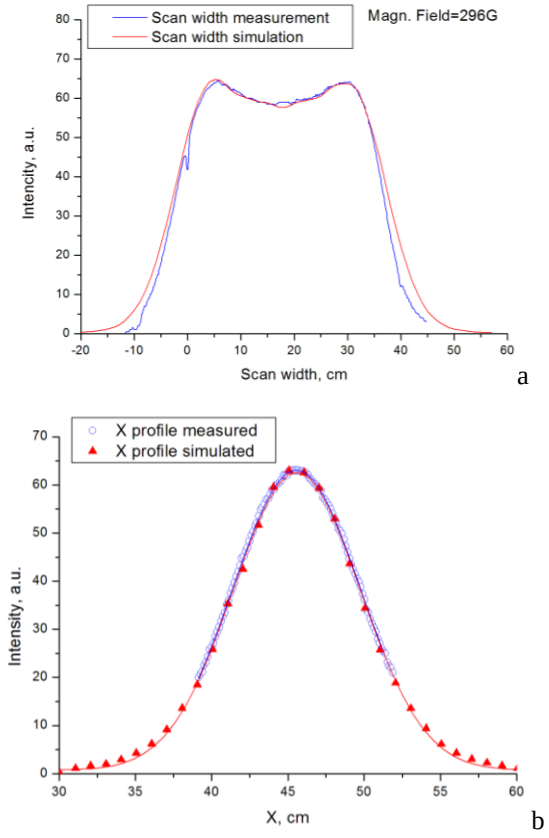


Fig. 13. Electron flux density distribution across the sweep on the radiator (a) and horizontal profile (b) for electron energy 9.7 MeV: blue line, blue circles – CL measurements; red line, red triangles – simulations (scaled)

2.3. MODEL VALIDATION AGAINST DEPTH-DOSE DATA

The simulated depth-dose distribution in a polystyrene phantom agrees well with the data of the independent measurements conducted on the 10 MeV IMPELA and "MeV Industrie S.A." accelerators [7] (Fig. 14), and with simulations using a ITS3 Monte Carlo code [8] over the range of beam energies (Fig. 15). A cross-check of absorbed energy and charge across the stack-monitor plates between Geant4 and Penelope code [9] agreed to within 5% (Fig. 16). Fig. 17 shows the simulated dose map in a polystyrene phantom (surface density 4 g/cm^2) irradiated with a 9.8 MeV scanning beam. It illustrates the combined vertical-sweep and depth-dose behavior, which can be used for the operational qualification of the irradiation process [10].

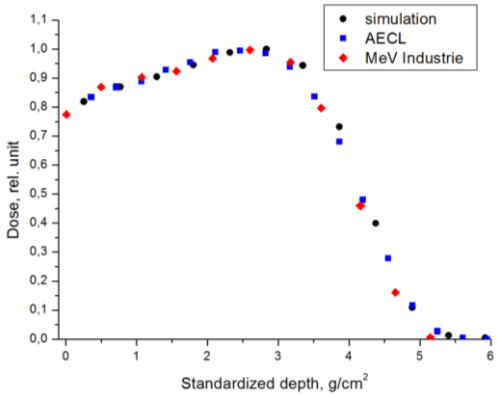


Fig. 14. Simulated depth-dose distribution (circles) vs. measured values on 10 MeV IMPELA (squares) and "MeV Industrie S.A." (diamonds) accelerators [7]

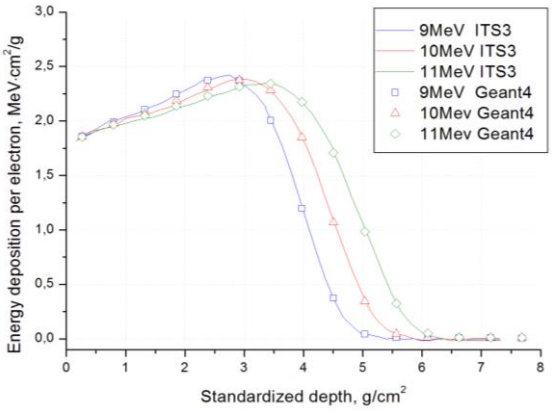


Fig. 15. Simulated depth-dose distribution in polystyrene for different beam energies, vs. the ITS3 code [8]

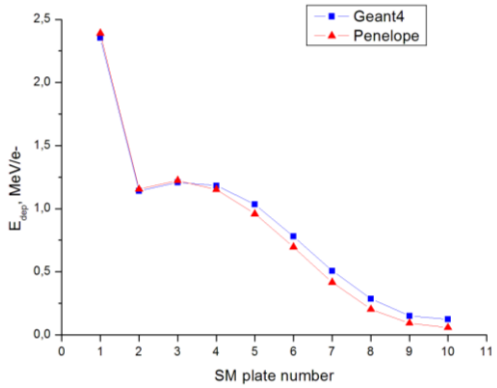


Fig. 16. Absorbed-energy distribution across the stack-monitor plates: Geant4 vs. Penelope, straight beam, 9.8 MeV

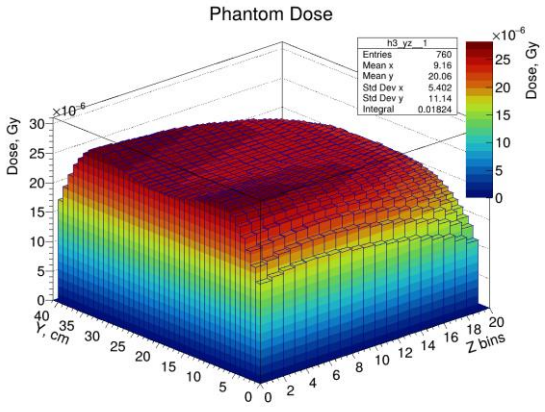


Fig. 17. Simulated dose map (vertical sweep vs. depth) in the polystyrene phantom, beam energy 9.8 MeV (Zbin=2 cm)

CONCLUSIONS

1. A Geant4 model of output devices of the LP-10 industrial accelerator was developed for simulating the dose distribution in an object irradiated by a scanning electron beam. Comparison with experimental data from LP-10, and also from other accelerators have shown that their deviations don't exceed 3%, confirming the model's accuracy and its suitability for planning and optimizing the conditions of the radiation processing.

2. The model accurately predicts the absorbed-dose distribution on the surface and within the volume of a processed object as a function of sweep width and beam energy, enabling virtual optimization of accelerator parameters before physical trials. This reduces the time and resources needed for equipment setup and is expected to improve the quality and cost-efficiency of industrial electron-beam treatment.

REFERENCES

1. V.I. Nikiforov, R.I. Pomatsalyuk, Yu.V. Rogov, V.A. Shevchenko, A.Eh. Tenishev, V.L. Uvarov. Development and Validation of Software for Simulation of Product Processing Regimes at an Electron Accelerator // *PAST. Series "Nuclear Physics Investigations".* 2013, N 6(58), p. 156-160.

2. V.N. Boriskin, S.A. Vanzha, V.N. Vereshchaka, etal. Development of radiation technologies and testsin "Accelerator" Sc&Res Est., NSC KIPT // *PAST. Series "Nuclear Physics Investigations".* 2008, N 5(50), p. 150-154.

3. R. Pomatsalyuk, S. Romanovskyi, V. Shevchenko, V. Uvarov. Real time luminescent dosimetry system for product processing at an electron accelerator // *PAST. Series "Nuclear Physics Investigations".* 2024, N 5(153), p. 131-135;
https://doi.org/10.46813/2024-153-131

4. S. Agostinelli et al. GEANT4 – a simulation toolkit // *Nucl. Instr. Meth. A*. 2003, v. 506, N 3, p. 250-303.

5. R.I. Pomatsalyuk et al. Measurement of electron beam energy characteristics at an industrial accelerator // *PAST. Series "Nuclear Physics Investigations".* 2017, N 6(112), p. 3-7.

6. A.N. Dovbnya, A.I. Kosoy, A.E. Tolstoy, V.A. Shendrik. Deflection and formation of the extracted beam of multipurpose electron accelerators at KIPT // *PAST. Series "Nuclear Physics Investigations".* 1997, N 1(28), p. 114-121.

7. ISO/ASTM 51649:2015(E), Standard Practice for Dosimetry in an Electron Beam Facility for Radiation Processing at Energies Between 300 keV and 25 MeV.

8. B.C. Franke, R.P. Kensek, T.W. Laub. ITS Version 5.0, Sandia National Laboratories, SAND2004-5172, 2005.

9. M. Cleland, R. Galloway, F. Genin, M. Lindholm. The use of dose and charge distributions in electron beam processing // *Radiat. Phys. Chem*. 2002, v. 63, N 3-6, p. 729-733.

10. ISO 11137-1:2025 Sterilization of health careproducts – RadiationPart 1: Requirements for the development, validation and routine control of a sterilization process for medical devices https://www.iso.org/obp/ui/en/#iso:std:iso:11137:-1:ed-2:v1:en.

Article received 01.09.2026

ПРОГРАМНИЙ КОМПЛЕКС ДЛЯ АНАЛІЗУ РЕЖИМУ ОБРОБКИ ПРОДУКЦІЇ НА ПРИСКОРЮВАЧІ ЕЛЕКТРОНІВ

Р. Помацалюк, С. Романовський, Д. Тітов, В. Титов, В. Уваров

Представлено результати експериментального дослідження та комп'ютерного моделювання розподілу поверхневої дози на об'єкті, що опромінюється сканованим пучком електронів промислового прискорювача LP-10 ННЦ ХФТІ. Розроблена на основі Монте-Карло коду Geant4 модель вихідних пристроїв прискорювача перевірена на відповідність експериментальним даним. Модельовані ширини розгортки пучка збігаються з експериментальними даними з похибкою 1…3%. Розраховані розподіли дози за глибиною об'єкта узгоджуються з даними, що одержані на інших прискорювачах, а також із результатами моделювання з використанням програм ITS3 та Penelope.